Natural Resources Canada
Ressources naturelles Canada

Slope-fan and glacial sedimentation on the central Beaufort continental slope, arctic Canada

K.M.M. Rohr, M. Riedel, S.R. Dallimore, and M.M. Côté

Geological Survey of Canada
Current Research 2021-1

2021

Canada

Geological Survey of Canada
Current Research 2021-1

Slope-fan and glacial sedimentation on the central Beaufort continental slope, arctic Canada

K.M.M. Rohr, M. Riedel, S.R. Dallimore, and M.M. Côté

2021

ISSN 1701-4387
ISBN 978-0-660-34934-3
Catalogue No. M44-2021/1E-PDF
https://doi.org/10.4095/326068

A copy of this publication is also available for reference in depository libraries across Canada through access to the Depository Services Program's Web site at http://dsp-psd.pwgsc.gc.ca.

This publication is available for free download through GEOSCAN (https://geoscan.nrcan.gc.ca).

Recommended citation

Rohr, K.M.M., Riedel, M., Dallimore, S.R., and Côté, M.M., 2021. Slope-fan and glacial sedimentation on the central Beaufort continental slope, arctic Canada; Geological Survey of Canada, Current Research 2021-1, 18 p. https://doi.org/10.4095/326068

Critical review

E. King
J. Dietrich

Authors

K.M.M. Rohr (kristin.rohr@canada.ca)
S.R. Dallimore (scott.dallimore@canada.ca)
M.M. Côté (michelle.cote@canada.ca)
Geological Survey of Canada
9860 West Saanich Road
Sidney, British Columbia
V8L 4B2

M. Riedel (mriedel@geomar.de)
Geological Survey of Canada
9860 West Saanich Road
Sidney, British Columbia
V8L 4B2

Present address:
GEOMAR Helmholtz Centre for Ocean Research
Kiel, Wischhofstraße 1-3, D-24148
Kiel, Germany

Correction date:

Slope-fan and glacial sedimentation on the central Beaufort continental slope, arctic Canada

K.M.M. Rohr, M. Riedel, S.R. Dallimore, and M.M. Côté

Rohr, K.M.M., Riedel, M., Dallimore, S.R., and Côté, M.M., 2021. Slope-fan and glacial sedimentation on the central Beaufort continental slope, arctic Canada; Geological Survey of Canada, Current Research 2021-1, 18 p. https://doi.org/10.4095/326068

Abstract: Quaternary sedimentary environments in the central Beaufort Sea continental slope are evaluated using interpretations of three–dimensional (3-D) seismic data. Previous knowledge of slope sedimentation has been limited to sparsely located, low-resolution vintage seismic-reflection profiles. The 3-D data image a number of channel-levee complexes that comprise a previously unknown slope fan we call the Kugmallit fan. The Kugmallit fan includes angular unconformities, and a broad spectrum of sediment deformation from coherent slide blocks and slumps to debris-flow deposits. The fan has been regionally truncated by a planar erosional unconformity overlain by laminar glaciomarine to hemipelagic sediments. This unconformity represents a significant change in depositional style, likely the result of reorganization of Plio–Pleistocene fluvial systems during the Last Glacial Maxima into the present day Mackenzie River drainage system. We infer that overpressure and fluid flow within the sediments in this slope fan are potential geohazards for exploration drilling.

Résumé : À l'aide d'interprétations de données sismiques tridimensionnelles (3D), nous avons évalué les milieux sédimentaires du Quaternaire de la partie centrale du talus continental de la mer de Beaufort. Les connaissances antérieures relatives à la sédimentation sur le talus reposaient sur un nombre limité d'anciens profils sismiques à faible résolution largement espacés. Les données 3D permettent de représenter un certain nombre de complexes de chenaux-levées, dont un cône de talus jusque-là inconnu auquel nous avons donné le nom de «cône de Kugmallit». Le cône de Kugmallit renferme des discordances angulaires et un large spectre de déformations sédimentaires allant de blocs cohérents de cônes d'éboulis et de structures d'affaissement à des dépôts de coulées de débris. Une discordance d'érosion plane recoupe le cône à l'échelle régionale et est recouverte de sédiments glaciomarins à hémipélagiques laminaires. Cette discordance témoigne d'un important changement du style de dépôt, qui résulte probablement de la réorganisation lors du dernier pléniglaciaire des systèmes fluviaux du Plio-Pléistocène ayant mené au système de drainage actuel du fleuve Mackenzie. Nous supposons que la surpression et l'écoulement des fluides à l'intérieur des sédiments de ce cône de talus constituent de possibles dangers géologiques pour les forages d'exploration.

INTRODUCTION

The near-surface sedimentary strata of the Canadian Beaufort Sea continental shelf have been extensively studied since the 1970s utilizing data from systematic two-dimensional (2-D) seismic surveys, geotechnical cores, and the results from more than 100 offshore hydrocarbon exploration wells (Pelletier, 1987; Blasco et al., 1990, 2013; Dixon et al., 1992; Dixon, 1996). However, knowledge of the subsurface sediments of the upper slope area is much more limited as there has been no drilling in water depths deeper than 85 m. Publicly available geophysical data sets in this area are restricted to scanned images of widely spaced 2-D multichannel seismic-reflection profiles collected 30 to 40 years ago. However, the outer shelf and upper slope of the Canadian Beaufort Sea are considered to be prospective hydrocarbon settings with a number of licences authorized for exploration by the Government of Canada in 2012 and 2013. While some preliminary investigations were conducted by industry on these exploration licences, in December 2016, the government announced that Canadian Arctic waters were to be indefinitely off limits to new offshore oil and gas exploration and development. Reconsideration of this decision was proposed to be undertaken every five years through a science-based review. This paper provides interpretations of the Quaternary geology of the central Beaufort slope, using 3-D seismic-reflection data acquired by industry and provided to the Geological Survey of Canada (GSC) for scientific studies. The central goal of the paper is to present a review of the seismic stratigraphy and geology of an extensive slope-fan complex that has not been previously described in the literature. This work extends our scientific knowledge of the area and contributes baseline information useful for the scientific assessment of the environmental consequences of possible continued hydrocarbon exploration in the upper slope areas of the Beaufort Sea.

GEOLOGICAL SETTING

Geomorphology

The study area is part of the upper continental slope in the central Beaufort Sea, north of the Tuktoyaktuk Peninsula and east of the Mackenzie Trough (Fig. 1). In the context of the Canada Basin, this region has been called the Mackenzie fan (Grantz et al., 1990; Jakobsson et al., 2003). Detailed multibeam bathymetry of the study area, (which also encompasses parts of exploration licences originally issued to Imperial Oil Resources Ventures Ltd. and BP Exploration Company Ltd.), was acquired through a collaborative initiative supported by Canadian industry and the ArcticNet research program (*see* University of New Brunswick Arctic Mapping Program available online at http://www.omg.unb.ca/arctic-mapping/). The shelf-to-slope transition occurs at about 110 m water depth and is 100 to 150 km offshore. The shelf edge trends in a southwest-northeast direction from the Mackenzie Trough in the west, to Amundsen Gulf in the east — a distance of 350 km. In the eastern part of our study area (Fig. 2) the shelf edge and the extended morphology in deeper water has a lobate shape. A similar, but less distinct, feature occurs in the western part of the study area. We call these features the Kugmallit and Ikit fans as they occur downslope of surficial valley features with the same names that have been identified on the shelf (Pelletier, 1987; Blasco et al., 2013). The surface morphologies of the two fans coalesce to form an extensive feature that is over 125 km long, extending from the shelf edge approximately 50 km offshore to water depths greater than 1000 m. The surface of the fans has been eroded by a series of coalesced slide scars, some of which intersect the shelf edge (Saint-Ange et al., 2014; Cameron and King, 2019). Several conical mud volcano features have been identified on the slope. These are active features which typically rise 10 to 30 m above the surrounding sea floor and are up to 500 m in diameter (Paull et al., 2015).

Regional stratigraphy and sedimentary environments

The geology of the immediate study area has not been previously described, but the stratigraphy of the shelf areas to the south and west was described by Dixon and Dietrich (1990), providing a basis for interpretation of seismic data. The youngest succession they describe consists of two main depositional sequences: the Pliocene to early Pleistocene Iperk Sequence and the Late Pleistocene Shallow Bay Sequence. The Iperk Sequence was characterized by rapid sediment deposition and progradation of paleo–shelf margins over older sedimentary strata that are part of a Tertiary-aged fold belt (Fig. 3) (Lane and Dietrich, 1995) and is defined seismically by its lack of large-scale tectonic folding and faulting. The Plio–Pleistocene succession is up to 4000 m thick beneath the north–central Beaufort shelf (Dixon and Dietrich, 1990; Dietrich et al., 2010; Graves et al., 2010), and thought to be 2500 to 4000 m thick beneath the slope area evaluated in this study (Helwig et al., 2015). A two-dimensional industry seismic profile (Fig. 3) illustrates a flat to gently dipping Late Miocene unconformity, overlain by the progradational Plio–Pleistocene succession. The Iperk Sequence, which occurs above this unconformity, is interpreted to consist of unconsolidated to weakly-cemented mudstone and sandstone. Depositional conditions are considered to be marine shelf and deep-water slope to basin plain settings (Dietrich et al., 1985; McNeil et al., 2001). Estimated sedimentation rates are high, varying from 400 to 600 m/Ma, which is up to 20 times higher than sedimentation rates estimated for older Miocene sequences (McNeil et al., 2001). As a consequence, the shelf edge is estimated to have prograded up to 120 km northward (Dietrich et al., 2010). In Figure 3, the oldest sediments have been truncated under the present-day slope and the youngest sediments have prograded over them (e.g. red line at 1500 m in Fig. 3).

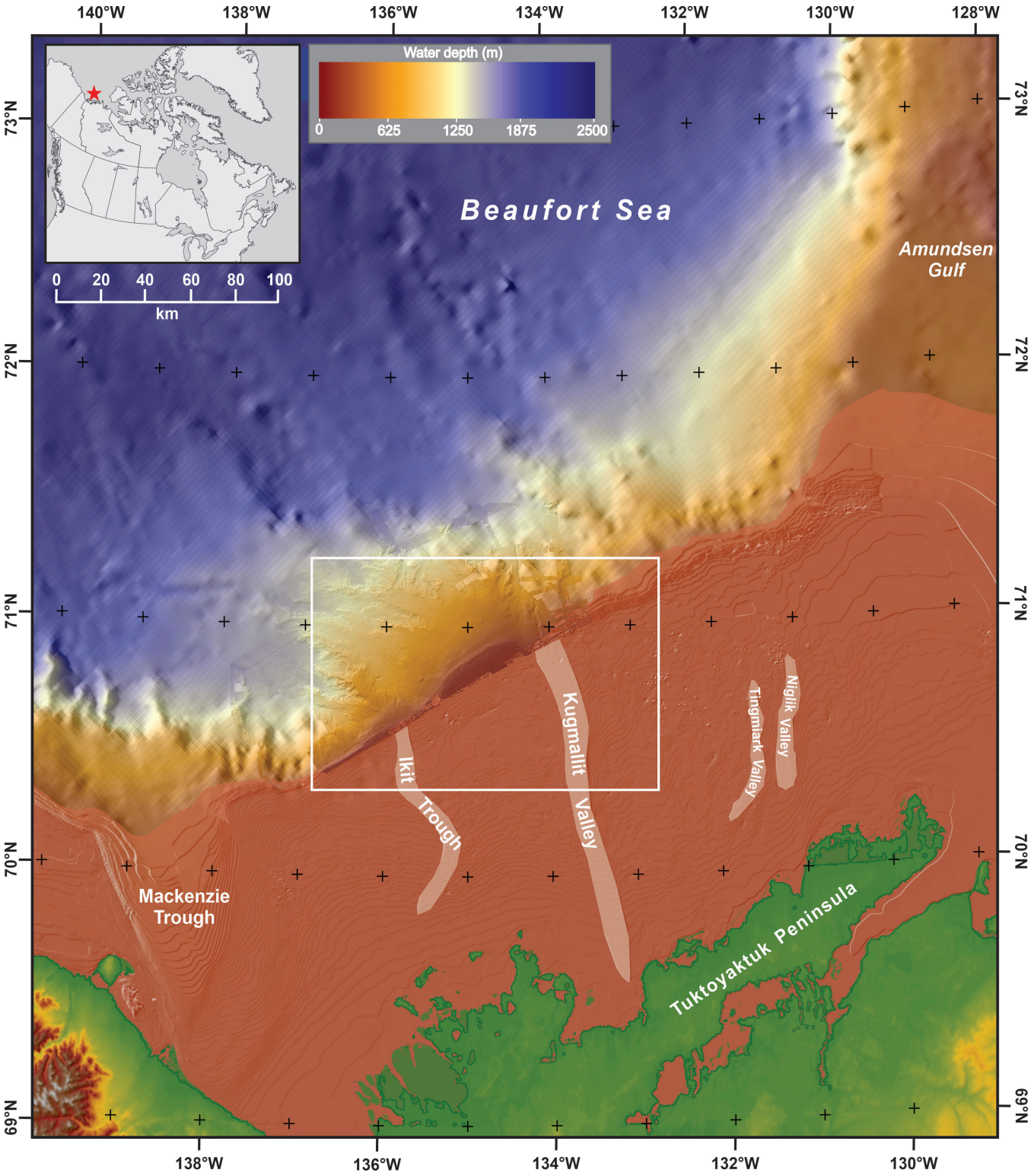

Figure 1. Regional bathymetry map of central Beaufort shelf and slope from the International Bathymetric Chart of the Arctic Ocean (http://www.ngdc.noaa.gov/mgg/bathymetry/arctic/arctic.html) and multibeam bathymetry. White box shows study area (Fig. 2). Valleys on the shelf are shown by beige overlay.

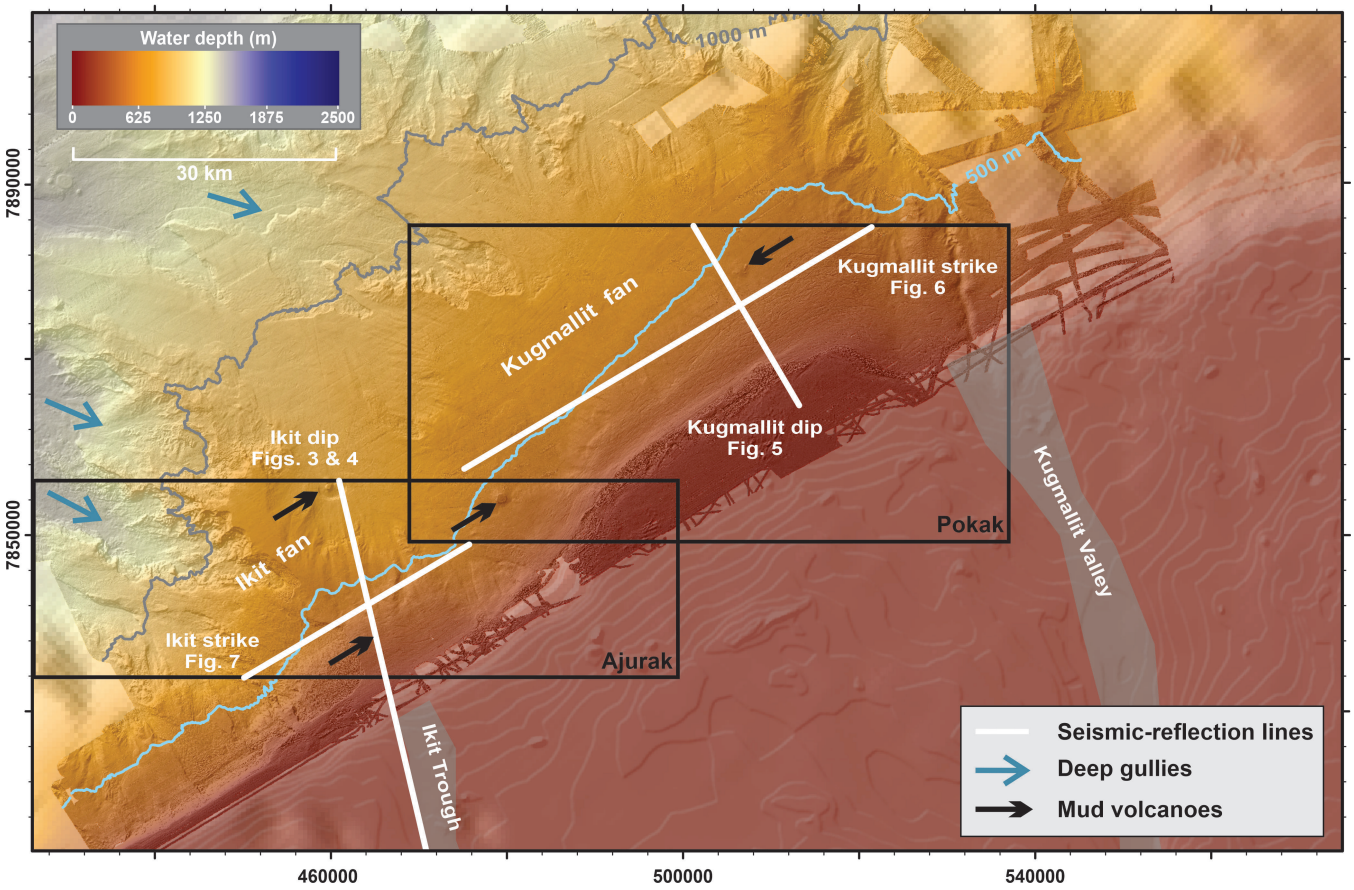

Figure 2. Multibeam bathymetry of the Beaufort-Mackenzie slope. The mouth of the Mackenzie Trough is 50 km to the west of the study area. Reflection lines discussed in the text are indicated by white lines. Valleys on the shelf are shown by grey overlay. The Ajurak and Pokak 3-D seismic-reflection volumes are show by black boxes.

The Shallow Bay Sequence is up to 400 m thick in the Mackenzie Trough, where it unconformably overlies Iperk and older strata (Dietrich et al., 1985; Dixon and Dietrich, 1990; Dixon et al., 1992) and consists of fine- and coarse-grained clastic sediments. Batchelor et al. (2014) have mapped seismic sequences using modern industry 2-D seismic data and have recognized possible evidence of two glacial tills which they infer could be a consequence of Wisconsinan or older glaciations. Identification of Shallow Bay strata in shelf areas is uncertain (Dixon and Dietrich, 1990; Dixon, 1996; Riedel et al., 2016), perhaps because it is too thin to be recognized on conventional 2-D seismic surveys. Interpretations of a research seismic line completed by the GSC (Line FGP-3) suggest that a thick wedge of Shallow Bay strata may be present beneath the slope seaward of the Mackenzie Trough (Dietrich et al., 2010); however, noisy data at the shelf break make linking that unconformity to the type section tills in the Mackenzie Trough difficult. No interpretations have been published from the lower resolution industry 2-D lines to the east.

The shallow surficial geology of the central Beaufort shelf was studied from industry geotechnical cores and high-resolution seismic profiles (Blasco et al., 1990). The complex and variable shelf sedimentary succession consists of regressive delta plain/delta front sands and finer grained transgressive muds (Riedel et al., 2021).

Several shallow unconformities have been identified in the top 150 m of sediments of the upper slope, based on interpretations from the 3-D seismic data sets described by Riedel et al. (work in progress, 2021) as well as in high-resolution 3.5 kHz data (Blasco et al., 1990). The recognition of megalineations associated with these unconformities suggests that they formed as a result of grounding of a glacial ice shelf (Riedel et al., 2021). Prior to these observations, the outer shelf and slope of the Beaufort Sea were thought to be beyond the limits of continental glaciation. The recognition of glacial features extends the area influenced by Quaternary glacial advances beyond the previously identified Mackenzie and Amundsen Gulf glacial troughs (Rampton, 1988; Vincent, 1983; Batchelor et al., 2013; Batchelor et al., 2014).

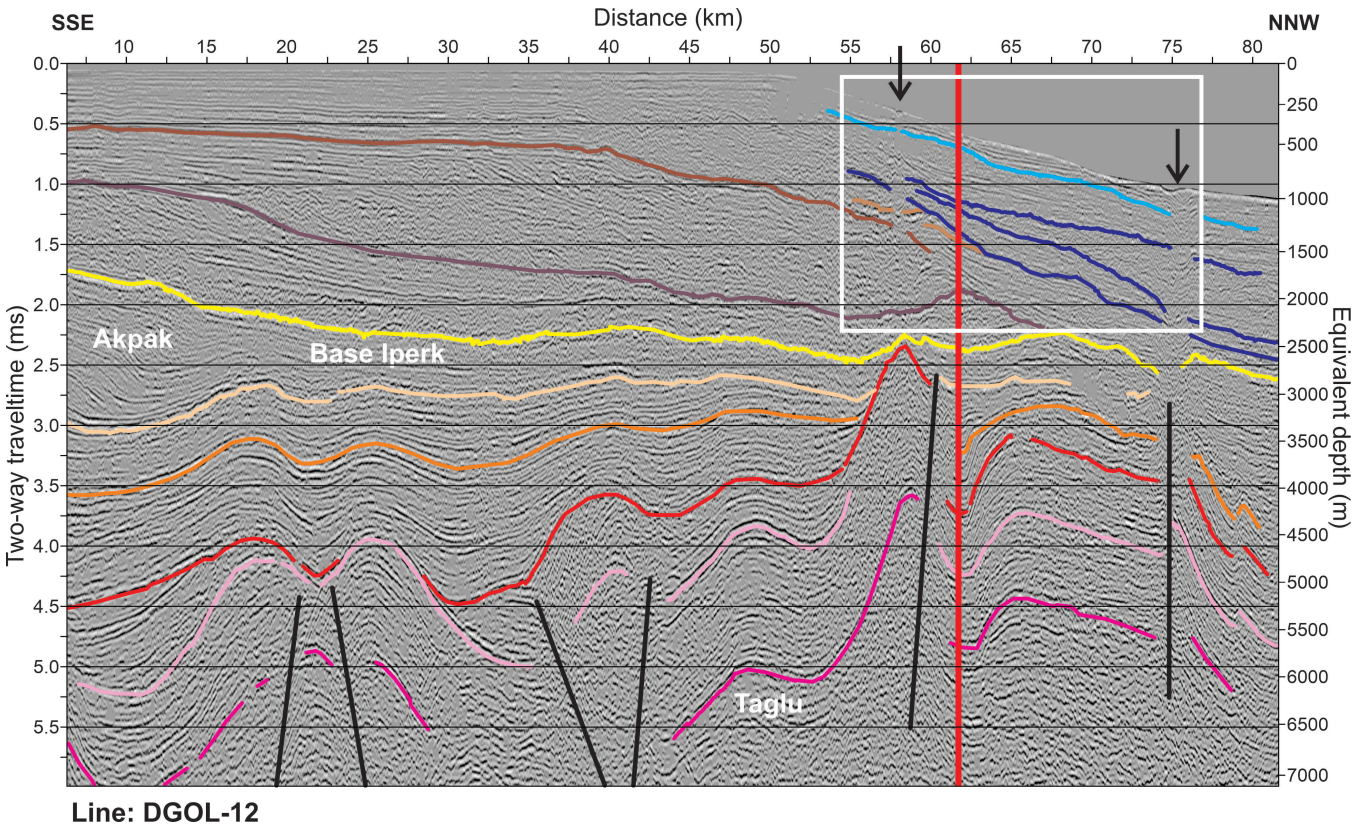

Figure 3. Ikit dip line crosses the continental shelf and slope showing a nearly flat base of the Iperk Sequence (yellow). Older strata, from the Miocene Akpak to the lower Eocene Taglu formations have been folded (Lane and Dietrich, 1995). Interpretations of the base of Iperk and older reflectors are slightly modified from Graves et al., (2010). Interpretations of prograding clinoforms within the Iperk Sequence are based on McNeil et al., (2001). Locations of mud volcanoes are indicated by black arrows. Blue horizons are unconformities interpreted in Figures 4 and 9. Vertical red line indicates the position of the Ikit strike line shown in Figure 9. White box shows data displayed in Figure 4. Line location is in Figure 2.

SEISMIC-REFLECTION DATA

The upper 2.2 to 2.7 s of the Ajurak and Pokak 3-D seismic-reflection data volumes were provided to the GSC by industry for geohazard and geological studies of the outer shelf and upper slope areas of the Beaufort Sea (Fig. 2). The Ajurak and Pokak 3-D data sets were acquired by Imperial Oil Resources Ltd. and BP Exploration Ltd., respectively; the data cover approximately 3500 km^2 of the upper slope with a narrow, irregular gap between the two data sets. The Ajurak data set had a dominant frequency of 50 Hz that permitted a resolution of 4.75 m at 1900 m/s and the Pokak data set had a dominant frequency of 40 Hz permitting a resolution of 5.9 m at 1900 m/s. Volumes of interval velocities were also provided to transform the migrated time data into depth. In describing the seismic sections, we refer to the x axis as distance in kilometres along the line and the vertical axis as metres below sea level.

A comparison between the publicly available 2-D multichannel lines (accessed through the archives of the National Energy Board) and a line from a 3-D volume along the track of DGOL-12 (Fig. 4a and b) illustrates the increased resolution and dynamic range of the 3-D data set. The 2-D data have a dominant frequency of 20 Hz compared to 50 Hz for the 3-D data. The 2.2 seconds of 3-D data show lateral and vertical variability in amplitudes that are not as apparent in the 2-D data. The vintage 2-D data were processed with an automatic gain function that smoothed out amplitude variations; for example, reflections below 1.2 s (0–5 km) have low amplitudes in the 3-D data that have been increased in the vintage data. Unconformities were interpreted on the 2-D data by comparison with the 3-D data; otherwise the interpretations were ambiguous. We do not have access to a velocity function for the 2-D data; therefore, Line DGOL-12 and its 3-D equivalent are shown as time sections.

INTERPRETATION

Regional correlations indicate that the 3-D data evaluated in this study images the Iperk Sequence above a Late Miocene unconformity (Fig. 3; Graves et al., 2010; Dietrich et al., 1985; 2010). The base of the Shallow Bay unconformity was not readily apparent in our assessment, largely because of the high degree of lateral discontinuity of strata.

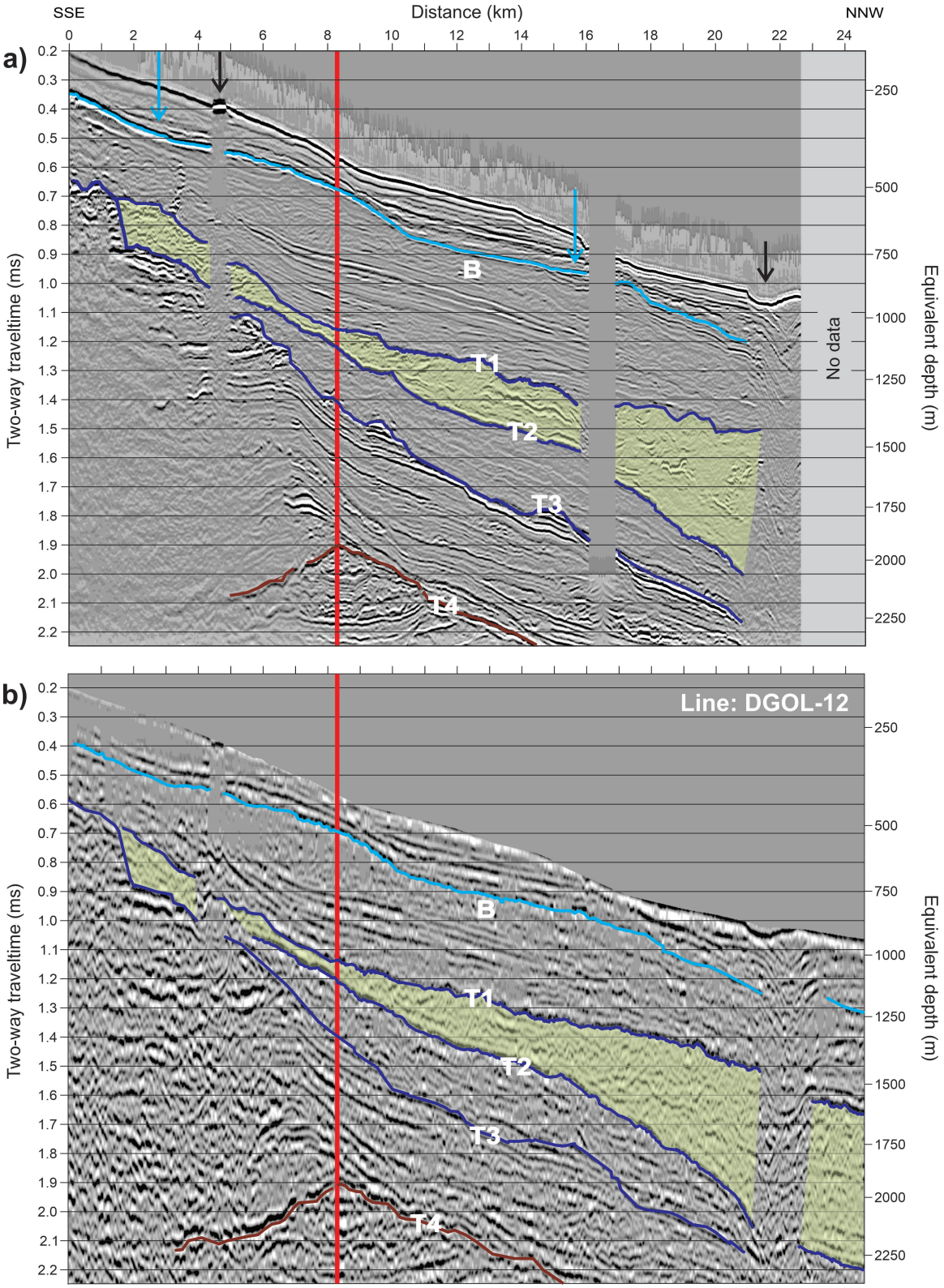

Figure 4. Comparison of time sections of seismic-reflection data along the Ikit dip line (Fig. 3). The sections are plotted at identical vertical and horizontal scales, with **a)** showing the 3-D seismic data and **b)** showing the publicly available 2-D line DGOL-0012 collected in 1979. During digitization from a paper record the seafloor reflector was clipped. The application of an automatic gain filter has smoothed out amplitude variations. Unconformities B, T1, T2 and T3 have been interpreted on the 3-D data and used as guidance to interpret the older data. Locations of mud volcanoes are indicated by black arrows. Blue arrows indicate extent of megalineations between 2.5 and 15.5 km, except for in the more steeply dipping area (9–10 km) where long lineations are not obvious. The vertical red line shows the intersection with the profile shown in Figure 9. Vertical exaggeration is 8:1. Line location is in Figure 2.

Interpretations of depositional environment, relative timing of deposition and of erosion are inferred mainly from seismic character, including bedding, shapes of sediment packages, contact relationships, as well as the occurrence of angular unconformities and evidence of sediment deformation. Seismic-reflection patterns in the 3-D data have some similarities to those observed in Quaternary continental slope settings from other regions (e.g. Posamentier and Kolla, 2003; Mayall et al., 2006, and references therein). We present for the first time an interpretation of depositional processes and environments in this area of the central Beaufort slope. The general seismic character of the various sediment packages is described; however, in this initial assessment we have refrained from mapping them out in detail.

Both 3-D seismic data volumes image clastic sedimentary systems which show evidence of a variety of depositional and post-depositional processes. Layered intervals are interpreted to indicate spatially uniform marine-sediment deposition while disrupted to chaotic intervals are interpreted as mass-transport deposits (MTDs) which comprise slide blocks, slumps, and debris flows (Richardson et al., 2011; Posamentier and Martinsen, 2011, and references therein). In some cases layered intervals transition downslope into MTDs. A widespread and continuous angular unconformity (B, seen in Fig. 4 to 6) overlain by a package of stratified sediments is imaged across the region at depths of approximately 80 to 100 m below the seafloor in deep-water settings; it then thins and ultimately pinches out near the shelf edge. Below this boundary, erosional unconformities are common throughout the full depth of the 3-D seismic volumes. However, they are spatially discontinuous and therefore, difficult to correlate. Multiple channel-levee complexes are apparent in the Ikit and Kugmallit fans as described in the following sections. The complexes are observed for tens of kilometres downslope from the present shelf break.

Kugmallit fan

Representative dip line

A dip line across the Kugmallit fan (Fig. 5) reveals seaward dipping packages of sedimentary strata that are characterized by parallel disrupted or chaotic reflections and low amplitude to nonreflective intervals. Four significant downslope-dipping, erosional unconformities (K3, K2, K1, and B) separate discrete sediment successions. Unconformities K3 to K1 are subparallel to the seafloor but have significant down dip relief of up to 100 m. Unconformity K2 is particularly abrupt at around 16 km along the dip line (Fig. 5) with 50 to 100 m of relief over less than a kilometre. Weakly reflective layers drape across the upslope and downslope edges of this scarp. A number of intervals with parallel seismic-reflections, suggesting uniform depositional conditions, can be identified with similar thicknesses downslope (e.g. the area shown by the yellow overlay in Fig. 5 and 6). However, sediments with disrupted or chaotic reflections vary more in thickness. A 100 m thick wedge of chaotic reflections above unconformity K2 between 2 and 16 km (green overlay, Fig. 5) is interpreted as a MTD that pinches out downslope against the eroded scarp in K2. In comparison, a thick section of slumped sediments interpreted between unconformities B and K1 thickens downslope. Unconformity B is laterally continuous beneath the slope but pinches out up dip at the shelf edge. Sediments above unconformity B are characterized by laterally continuous parallel seismic-reflections interpreted to represent uniform marine depositional conditions.

Representative strike line

A strike line across the Kugmallit Fan (Fig. 6) reveals the complexity of the geological setting and allows more detailed interpretation of sedimentary environments represented. The section images four sediment packages that have seismic characteristics consistent with the interpretation as channel-levee complexes described in other settings (e.g. Pacht et al., 1992; Posamentier and Kolla, 2003; Mayall et al., 2006, and references therein; Pickering and Hiscott, 2016). Channels are recognized in vertical seismic sections by concave upward, intermittent to chaotic bright reflections and in horizontal slices by their long sinuous shapes. Sediments along deep-water channel thalwegs are typically compositionally heterogeneous, ranging from sand to mud which creates high impedance contrasts and bright reflectors. In strike profiles, levees are usually recognized as wedge-shaped sediment packages that thin and downlap away from a channel; the finer grained sediments of the levees appear seismically as subparallel weakly reflective units. Levee depositional environments include overbank, splay crevasse, and distal turbidites deposits.

Three channel-levee sediment complexes and one channel cut into MTDs have been interpreted on the Kugmallit strike line (Fig. 6). Each of these channel-levee complexes has associated abrupt angular unconformities (K1, K2, and K3) that are broadly convex, with the highest parts occurring over interpreted channel complexes. They step down across the levees with up to 300 m of incision into underlying strata. For example, unconformity K2 cuts steeply down through an underlying levee complex on the northeast side of a channel (47 km, 800–1100 m depth, Fig. 6). Layered low-reflectivity intervals and numerous chaotically bedded intervals are commonly interpreted as MTDs. A shallow erosional unconformity (B) cuts across the entire section and is overlain by seafloor conformal strata.

The lowermost channel has an hourglass shape in cross-section and is bracketed by symmetric normal faults indicating possible sediment collapse into the channel (Fig. 6). Sediments surrounding these levees are deformed and overlain by a layered unit containing high-amplitude subparallel reflections. The channel-levee complex below unconformity K3 lies above a 100 to 200 m thick interval of deformed sediments. The northeastern side of the

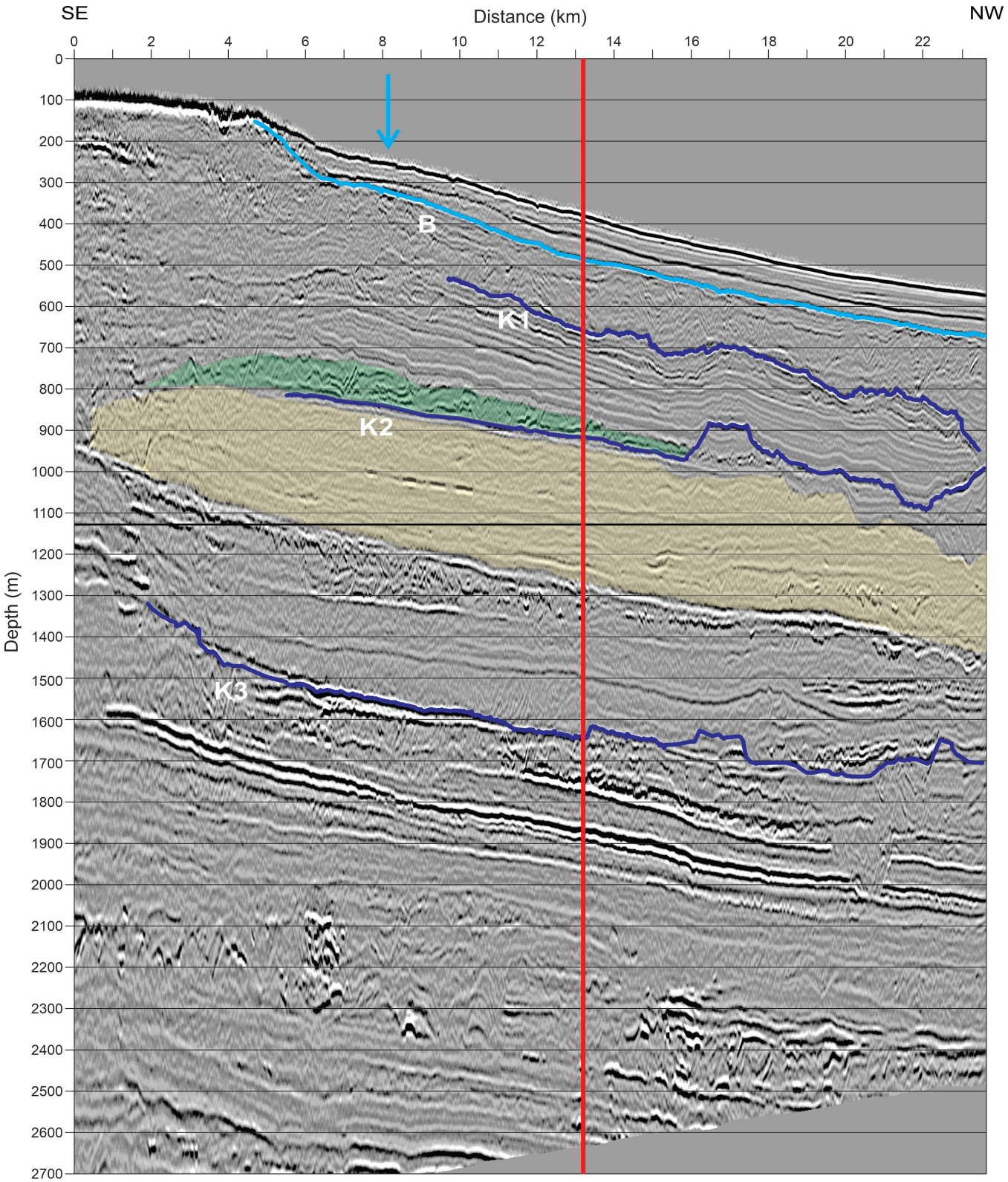

Figure 5. Representative dip line from the Pokak 3-D volume across the eastern slope of the Kugmallit channel shown as a depth section. The dark blue lines indicate angular unconformities; yellow colour indicates levee deposits interpreted in the strike line (Fig. 6). The green overlay indicates MTD. The blue arrow is the updip limit of the megalineations. The vertical red line shows intersection with line in Figure 6. Vertical exaggeration is 11:1. Line location is in Figure 2.

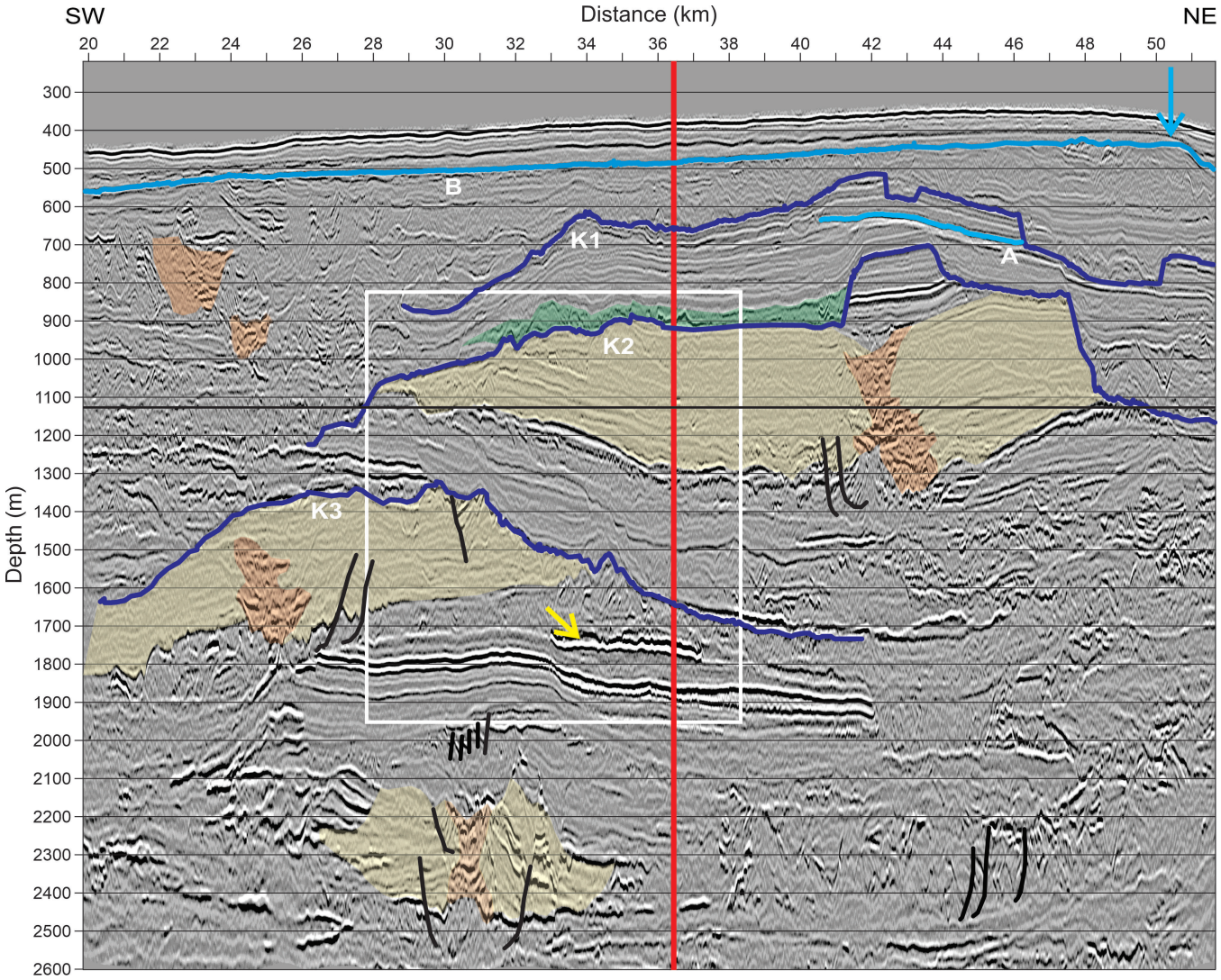

Figure 6. Representative strike line from the Pokak 3-D volume across the Kugmallit fan shown as a depth section. Pale orange indicates channel sands; yellow indicates levees, short black lines indicate faults and blue lines indicate angular unconformities. Unconformities A and B (light blue reflectors) have been interpreted by Riedel et al. (work in progress, 2021) to be scored by glacial megalineations. Yellow arrow points to a high-amplitude reflection and the blue arrow indicates the northeastern limit of megalineations. Thin black line at 1125 m indicates depth of horizontal slice across the volume shown in Figure 8. Vertical red line shows location of seismic line in Figure 5. The white box outlines data shown in Figure 7. Vertical exaggeration is 11:1. Line location is in Figure 2.

complex is cut by a number of normal faults (39 km, 1300–1400 m depth, Fig. 6), indicating that the levee failed before deposition of the overlying layered interval. The large channel-levee complex under unconformity K2 is up to 15 km wide. These levees have collapsed both inwards toward the channel as well as outward on the levee edges (Fig. 6). The shallowest channel has been cut into a volume of MTDs; further downslope levees formed on either side of it. Two remarkably bright laterally coherent reflections (Fig. 7, horizontally at 1800–1850 m depth) stand out in the strike line when compared to the largely transparent intervals that are adjacent to them. The shallowest of these intervals increases sixfold in amplitude (Fig. 7). This magnitude of increase is unlikely to be caused by variations in grain size or composition and is interpreted to possibly result from unusual formation conditions, such as overpressure. Sediment deformation ranges in style from coherent blocks to debris flows and can be seen at all depth intervals of the seismic-reflection data. Mass-transport deposits dominate the lower half of the northeastern end and the upper half of the southwestern side of the Kugmallit strike section.

In the Kugmallit strike line, unconformity B is a subhorizontal surface, generally conformal to the seafloor. It has a grooved surface that has been interpreted to have been formed by grounding of a glacial ice sheet (Riedel et al., in press;

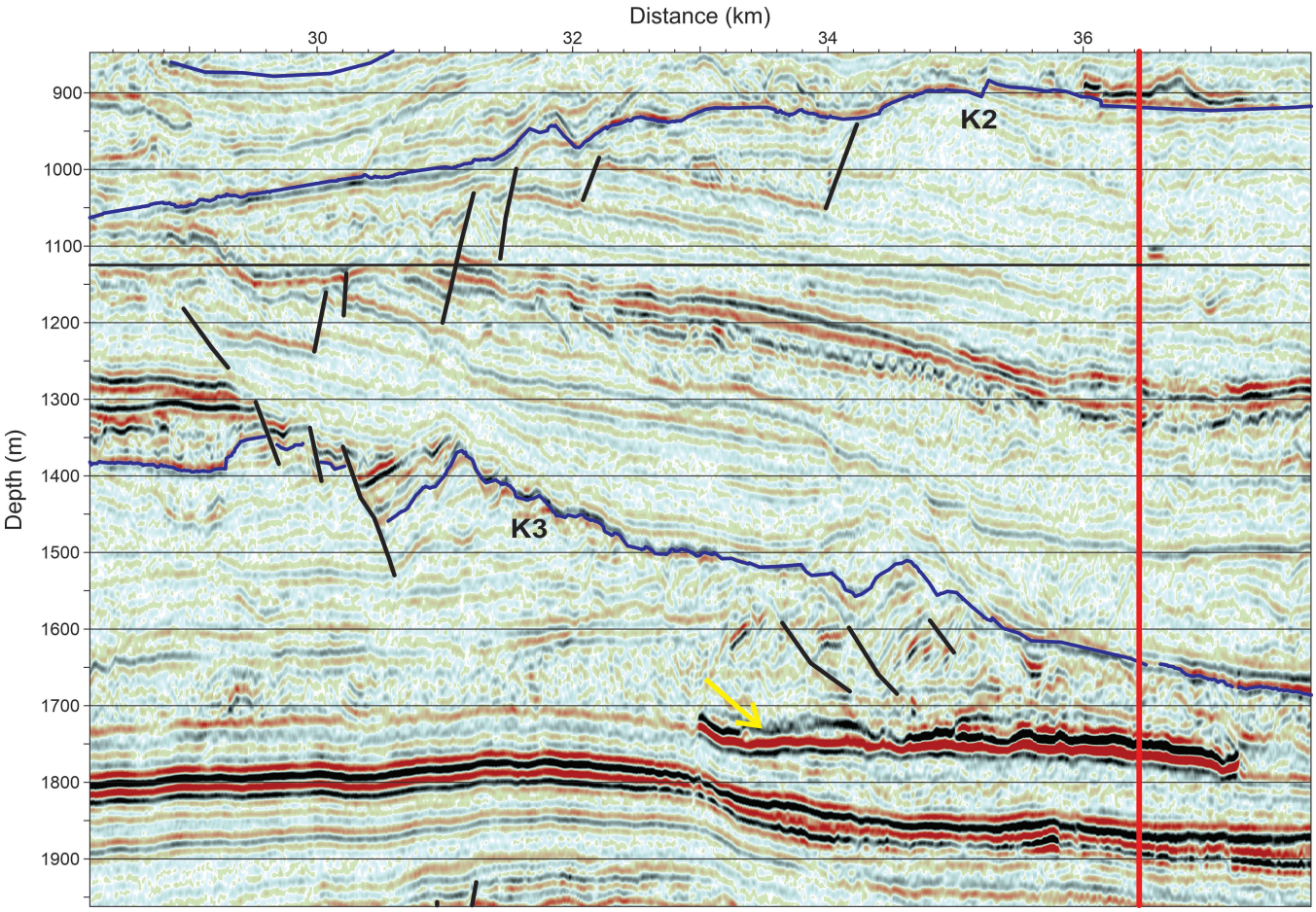

Figure 7. Detail of seismic section shown in Figure 6. Reflector at about 1750 m (yellow arrow) brightens by a factor of 6 underneath slides associated with this channel-levee complex. Thin line at 1125 m indicates depth of horizontal slice across the volume (Fig. 8). Vertical exaggeration is 6:1.

Woodworth-Lynas et al., 2016a,b). Unconformity A, a local feature on a paleotopographic high, is also grooved and interpreted to have formed in a similar manner. A MTD up to 200 m thick with contorted reflectors is recognized beneath unconformity B.

Lateral extent of channels

Depth slice sections through the 3-D seismic volumes are particularly useful for revealing the lateral continuity of channel sequences seen in strike lines. For example, a depth slice at 1125 m shows channel sequences of the Kugmallit fan (Fig. 8) as curvilinear bands of bright reflections. A long channel feature apparent in the eastern portion of the survey area is approximately 1 to 2 km wide and trends sinuously downslope. Generalized plan views of channels (Fig. 9) were derived from interpretations of multiple depth slices. The channels occur in a zone 70 km along strike beneath the slope; the central group of four channels appear to radiate from a location under the present shelf edge. The single identifiable channel in the Ikit area is only 1 km wide and is overlain by the failed edge of a gully.

Ikit fan

Representative dip line

As observed in the Kugmallit fan, a dip line across the Ikit fan (Fig. 4a) reveals seaward-dipping packages of sedimentary strata that are variably characterized by parallel seismic-reflections, disrupted or chaotic reflections and low amplitude to nonreflective intervals. Five significant downslope-dipping, erosional unconformities (T4, T3, T2, T1, and B) separate discrete sediment successions. The lowermost unconformity T4, is near the base of the truncated seismic data set provided for our research and was identified only in part of the survey area. Imaging of sediments below T4 is therefore rather poor. The entire sediment complex above unconformity T4 is well imaged and in our view, comprises a sedimentary succession consistent with a slope-fan complex that we call the Ikit fan. Sediments between T4 and T3 unconformities are up to approximately 400 m thick. For the most part they are characterized by laterally continuous, parallel seismic-reflections with gentle downslope dip angles. However, there are sediment packages with varying dip angles and chaotic bedding that are characteristics

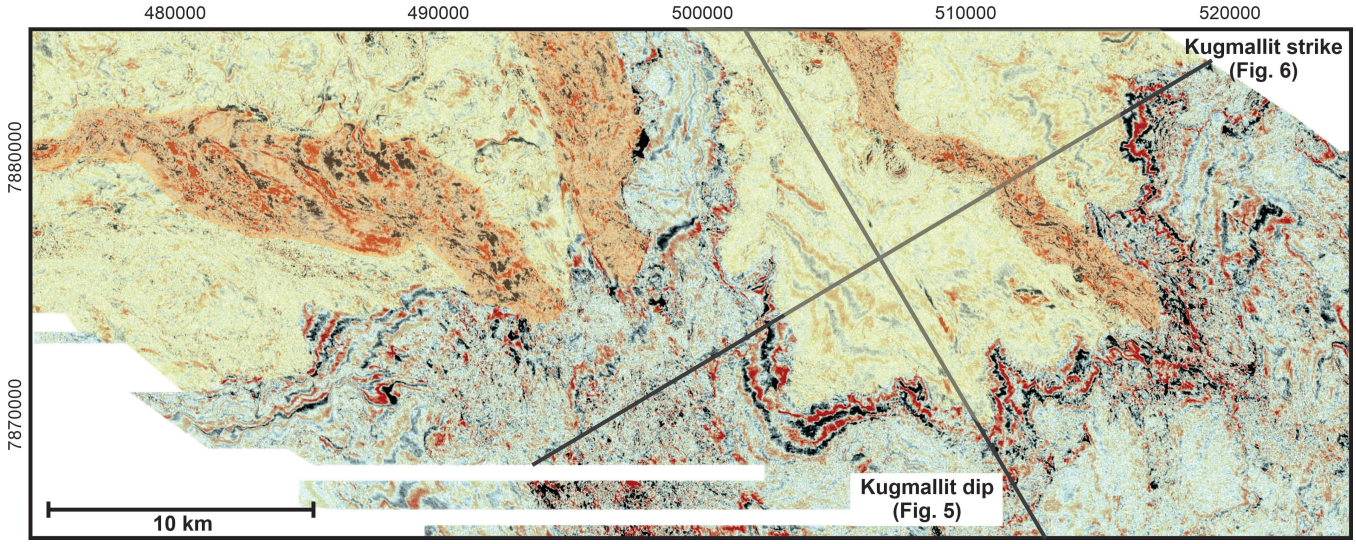

Figure 8. Depth slice across the Kugmallit fan taken at 1125 m. Orange overlay indicates channel sands while the yellow overlay indicates levee deposits. Locations of the representative Kugmallit dip and strike lines (Fig. 5 and 6) are shown in grey.

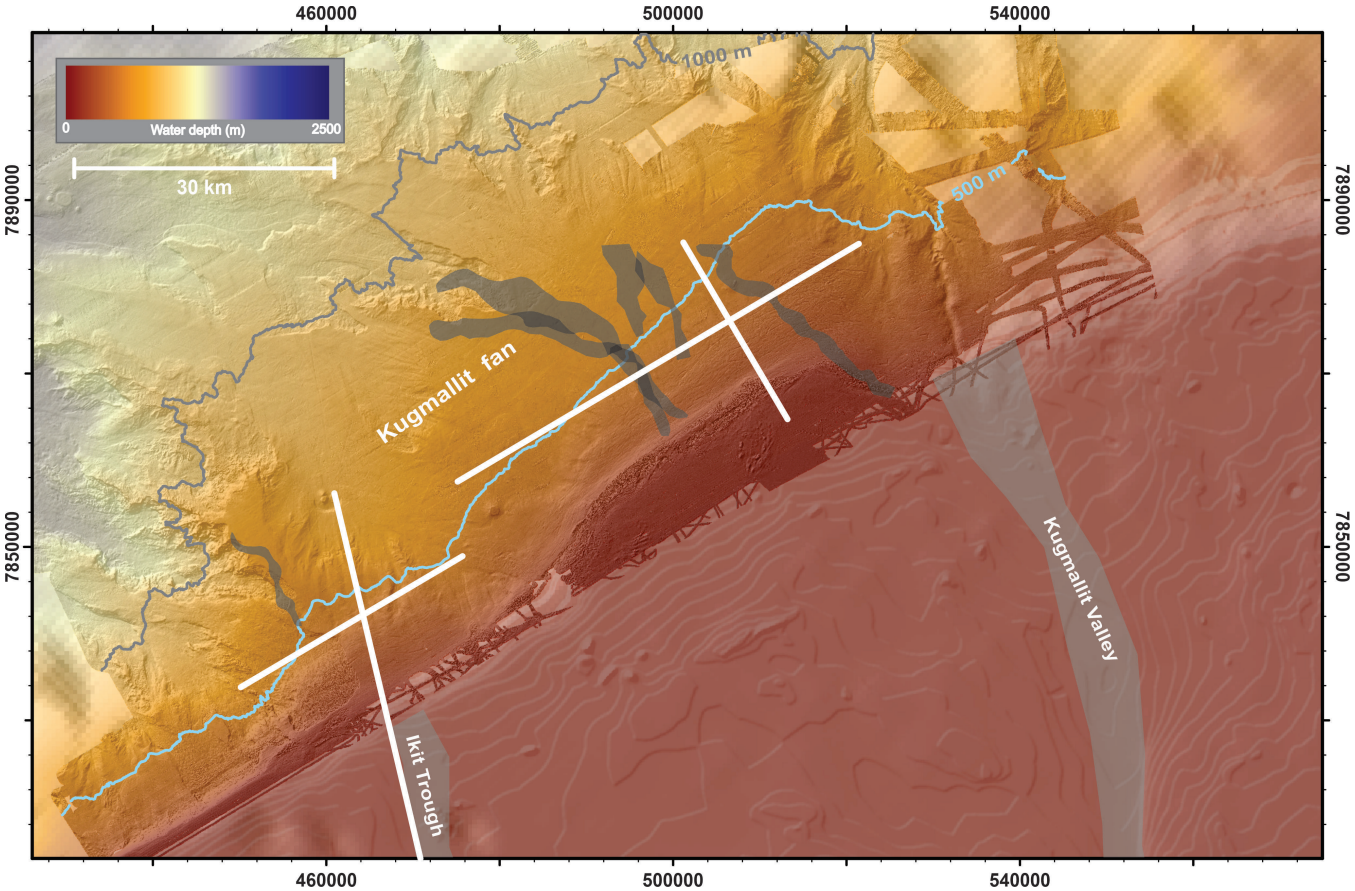

Figure 9. Generalized locations of channels (shown as dark grey overlays) interpreted in Figures 6 and 8.

typical of MTDs. Sediments between T3 and T2 are laterally continuous but transparent to weakly reflective when compared to the sediments below. The T2 unconformity merges with the T3 unconformity at around 1000 m sub-bottom depth. Sediments above unconformity T2 have folded and chaotic seismic character, and thicken rapidly downslope where they are more than 500 m thick. These characteristics indicate that, at the location of this dip line, sediments in this interval comprise a complex of MTDs, which cut into the lower sediments at depth. Sediments between unconformity T1 and B have variable seismic character with laterally parallel reflections dominating the lower part of the sediments, and chaotic, nonreflective character in the upper part more typical of MTDs. While there is considerable evidence of erosion and MTDs throughout the entire sediment succession of the Ikit fan, these processes appear to be confined to specific sediment packages. We see no evidence of tectonic deformation or faulting as is obvious at depth beneath the base of the Iperk Sequence (Fig. 3). Two mud volcanoes imaged on the dip section shown in Figure 4 (black arrows) may have been formed by fluid and gas migration from depths greater than 750 m (Paull et al., 2015). Both overlie faulted anticlines just below the base of the Iperk Sequence (Fig 3). Reflection amplitudes are significantly reduced below these features (Fig. 4a), most likely due to the presence of gas in the sediments. Bright spots are prevalent under unconformity T3 from 0 to 7 km and amplitudes are dimmed below them. Both of these characteristics can be interpreted as indications that free gas is present.

From approximately 3 km (~250 m water depth and 200 m burial depth) to 16 km (950 m water depth and 150 m burial depth) along this dip line, unconformity B has parallel grooves which trend in a northeast-southwest orientation (Fig. 4a). These have been interpreted as glacial megalineations (Riedel et al., in press; Woodworth-Lynas et al., 2016a,b). Unconformity B thins toward the shelf edge and continues to dip downslope below the grooved interval possibly suggesting a contact depth for the grounded ice shelf. Above this, reflections are mostly subparallel to the seafloor which is thought to indicate stable slope deposition of glaciomarine and marine sediments.

Representative strike line

The strike line crossing the Ikit fan (Fig. 10) reveals complexity in the sedimentary section that is not readily apparent in the dip line (Fig. 4). The deeper unconformities (T1, T2 and T3) are undulating to locally steeply dipping and show remarkable relief that is sometimes >300 m. The deepest unconformity, T4, is only visible over a few kilometres near the base of the section. The unconformities do not parallel each other but seem to have formed as completely separate and very substantial erosional events. Some sediment intervals above the unconformities have parallel, low-amplitude reflections of variable dip directions that are consistent with sediment drape above the unconformity surfaces (e.g. above T1 from 12–14 km). In other intervals, significant post-depositional slumping or sliding has occurred (e.g. below T2, 4.5–6 km).

Sediments below unconformity T3 with parallel bedding change dip along the line and become more reflective from west to east. Several intervals, for example 1750 m depth at 18 km, contain high amplitude reflections that are on the order of 1 to 2 km wide (Fig. 10). Unconformity T3 itself is a high-relief surface, with relief of 150 m between 8 and 9.5 km and up to 400 m between 9.5 and 13 km. The sediment package between unconformity T3 and T2 also shows significant complexity (Fig. 10). A distinct and widespread chaotic interval interpreted as a MTD directly overlies unconformity T3 in the west (0–9 km, green overlay), whereas in the east the interval is weakly reflective and conformable to the unconformity. A thick package of intermittent high-amplitude reflections (between 8 and 13 km, approximately 900–1200 metres below sea level) is interpreted as a channel-levee complex (orange transparent overlay). In this interval, high-amplitude reflections appear to form a syncline 200 m deep. Unconformity T2 has even higher relief than unconformity T3, with approximately 600 m of relief from 11 to 18.5 km. A chaotic interval interpreted to be a MTD (green overlay) occurs in this depression and can be traced downslope to the northwest (Fig. 4). Above unconformity T1 low amplitude reflections are largely conformal to the unconformity, but are truncated by unconformity B between 11 and 20 km.

Unconformity B is planar where grooved with glacial megalineations (0–5.5 and 10–17 km) (Riedel et al., in press; Woodworth-Lynas et al., 2016a,b), but undulates in depth to the east (between 20 and 30 km, Fig. 10). In addition, between 5.5 and 10 km it forms a broad valley which is approximately 200 m deep and 4.5 km wide. Sediments above this part of the unconformity are somewhat chaotically bedded but appear to infill the valley feature with similar slopes to the valley walls. These observations are further evidence of keel depth of the ice shelf.

At 11.5 km surficial sediments have failed to the west, forming a feature called the Ikit slump (i.e. Saint-Ange et al., 2014). Layered beds below the seafloor become transparent under the surficial expression of the slide and a reflector between 30 and 100 m below seafloor is contorted into folds about 200 m in wavelength and 10 to 20 m in height.

DISCUSSION

Slope-fan deposition

The seismic-reflection data enable interpretations of a dynamic depositional environment with large volumes of sediment being transported to the upper continental slope. We interpret that much of the sedimentary succession in the study area consists of slope channel-levee complexes that possibly formed as two coalesced, mixed mud and

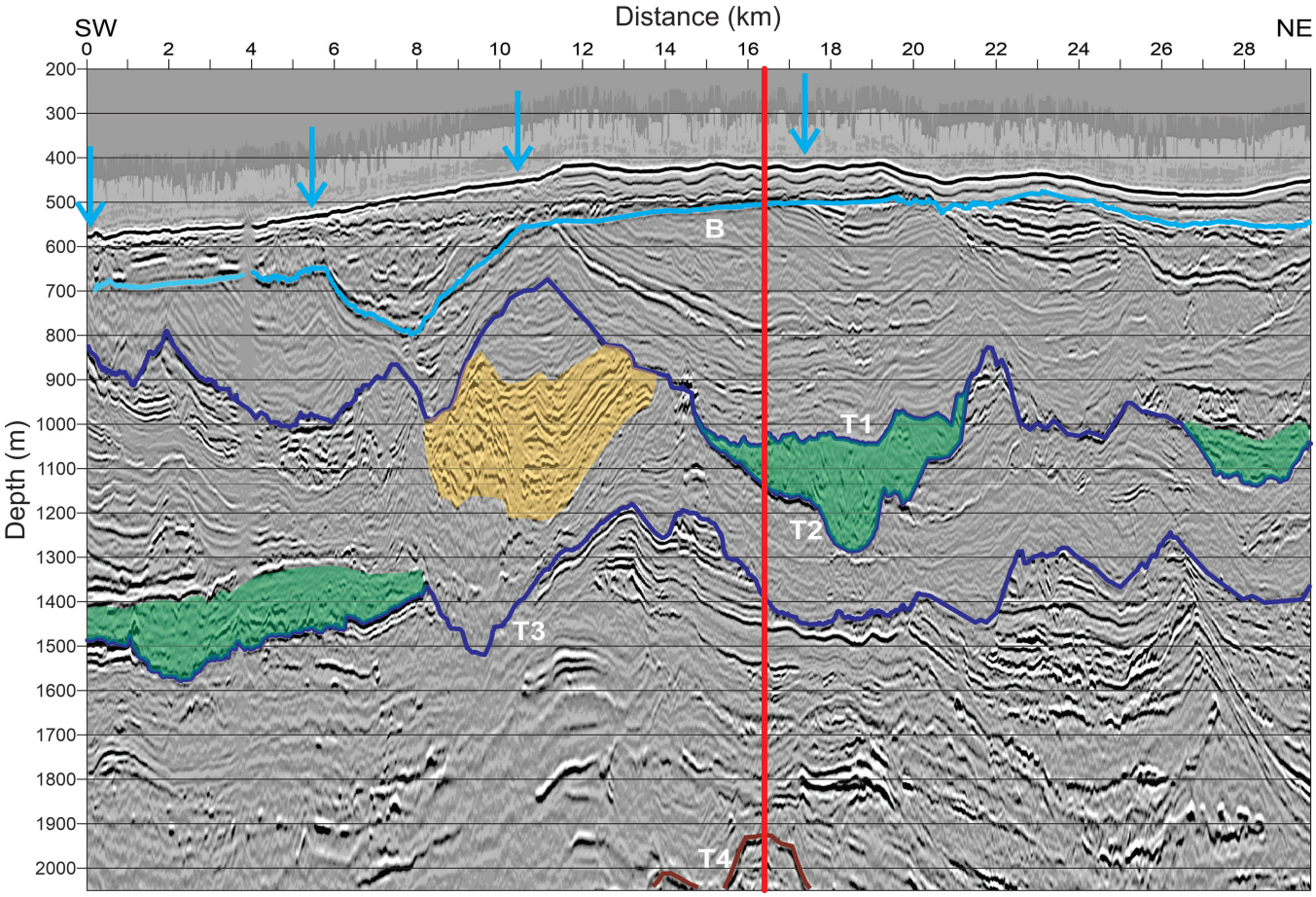

Figure 10. Representative strike line in the Ikit area which shows layered sediments and MTDs (green overlays), with orange overlays indicating channel sands. Unconformities B, T1, T2 and T3 are shown as blue horizons. Megalineations occur on unconformity B where it is flat as indicated by blue arrows from the southwestern edge of the section to 5.5 km and from 10.5 to 17.5 km. The vertical red line is intersection of dip line in Figures 3 and 4; line locations are in Figure 2. Vertical exaggeration is 11:1. Note that this is a depth section and the dip line is a time section (to allow for comparison with legacy data). As indicated in the text, lateral variability in reflections amplitudes is common.

sand slope fans (Vail, 1987) (Fig. 11). Seismic-reflection records from the proximal and distal areas of the fans reveal classic geometry and reflection characteristics of channel fill, levees, overbank deposits, as well as slumps and debris flows as described by numerous authors (i.e. Flood et al., 1991; Posamentier and Kolla, 2003; Posamentier and Martinsen, 2011; Weimer and Slatt, 2007; Sawyer et al., 2007; Pickering and Hiscott, 2016). Variable reflection amplitudes along a reflector are evidence of lateral changes in lithology, porosity, and/or fluid pressure. Individual channel-fill deposits are up to 300 m thick as are adjacent levee deposits. The regional significance of the fan features themselves is revealed in part by their extent. The coalesced fans extend about 120 km in length along the upper slope and more than 50 km downslope to the edge of the seismic data sets we have investigated. The sediment packages making up the fan are more than 1.5 km thick and assuming that they extend to deeper waters, they likely make up greater than 10 000 km^3 of sediment.

Evidence of widespread slumping and normal faulting indicate that the channel-levee complexes were very unstable features. Channel walls are often deformed by small offset normal faults which cut down into surrounding levees and underlying sediments (Fig. 6). Failure of channel walls is thought to be a typical feature of high-sedimentation-rate environments (e.g. Jobe et al., 2011 and references therein; Sawyer et al., 2014). In the Gulf of Mexico, channel-wall failure deforms sediments up to 10 km on either sides of channels (Sawyer et al., 2007). In Figure 7, such deformation can be seen to distances of 5 to 10 km further downslope. In some parts of the Kugmallit fan, there appears to be a relationship between the channel-levee complexes and overlying MTDs. For example, the apices of unconformities K1 and K2 overly the channel at around 1000 m depth (Fig. 6) and both unconformities step down away from the apex. K2 is overlain by a thin MTD to the southwest and K1 is overlain by a very thick sequence of MTDs. The abrupt step-wise shape of the K1 unconformity is likely related to slope failure

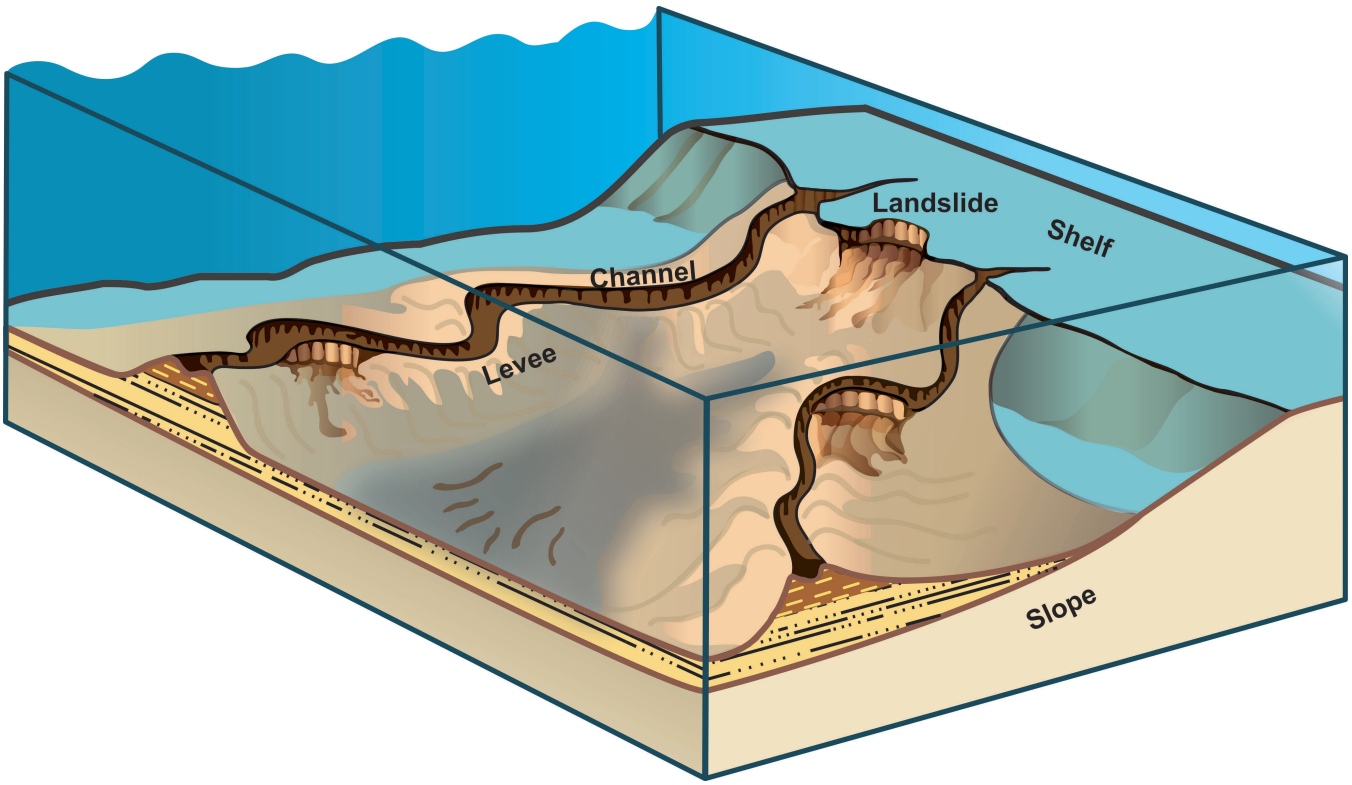

Figure 11. Schematic block diagram showing evolution of sinuous channel–levee systems on the continental slope. Channels can originate at different locations on the shelf; levees build up on either side. Landslides along the shelf edge generate debris flows. Failures along the levees can also generate debris flows.

(e.g. 42–43 km and 46–50 km, Fig. 6) although little of the failed material is obvious in this section. These observations suggest that lateral failure has occurred on either side of the channel-levee crests likely influenced by the rapid buildup of levee topography during high-energy sediment flows down the channel.

Our interpretations suggest the Kugmallit fan succession developed through cycles of channel-levee deposition, with vertical aggradation, and avulsion of channel complexes with some lateral migration though time (Fig. 8). High-amplitude reflections at the base of levees (Fig. 6 and 7) may arise from sandy layers deposited during unconfined flow from events such as avulsion or levee failure; once levees have been re-established, such coarse sediments would flow down the channel to be deposited downdip (Posamentier and Kolla, 2003; Flood et al., 1991). We interpret the Ikit fan to be more dominated by gully formation and overbank deposition. Low-amplitude to nonreflective intervals which drape over unconformities T2 and T3 are possibly indicative of turbidite-flow deposits. Deeply incised unconformities, and debris flows infilling low regions above unconformities indicate that erosion and mass transport were important processes and were likely influenced by high sedimentation rates. The single channel-levee complex identified in the Ikit area is 45 km distant from the channel-levee sequences seen in the Kugmallit area. This suggests that sediment input forming the two fan complexes came from more than one source channel on the shelf. However, the two fans have coalesced downslope.

Age considerations

Quaternary slope channel-levee complexes have been recognized in other continental slope settings in North America and Europe and are thought to have formed during sea-level low stands (i.e. glacial maxima) (Vail, 1987; Posamentier and Kolla, 2003; Hesse et al., 1999; Rydningen et al., 2016), especially as glaciers melted. In the Mars–Ursa region of the Gulf of Mexico, four different channel-levee complexes have been deposited during the last 70 000 years (Sawyer et al., 2007). The setting in our study area is at the northern terminus of the Laurentide Ice Sheet which covered much of North America. Repeated glaciations during the Quaternary would be expected to contribute substantive glaciofluvial discharge and large sediment supply to the outer continental shelf and upper slope. While definitive age assignment of the slope fan features we describe is problematic without coring or better regional correlation, our assessment is that they are likely of Quaternary age. Fluctuating sea level and glaciofluvial runoff likely greatly affected the progradation of the fans. Sediment supply was almost certainly reduced during interglacial periods when sea level was high, creating conditions more conducive to hemipelagic sedimentation. During

glacial times, sea level would be lower with potential for very rapid sedimentation rates. The deeply incised and discordant unconformities indicate periods of significant erosion, perhaps even indicating glaciofluvial outburst events such as described by Murton et al. (2010). The abundant MTDs and localized faulting of channel/levee sediments indicate significant slope and sediment instability. The complexity of the glacial setting in the outer Beaufort shelf and upper slope is only now being revealed.

It is generally considered that continental glacial ice did not reach the shelf edge at least in the last glaciation (e.g. Rampton, 1988; Dyke et al., 2002) and no glacial tills have been identified in wells drilled on the shelf (Blasco et al., 1990). Large variations in sea level are known to have occurred and are associated with significant variations in lithofacies (Hill et al., 1993; Picard, 2012). Glacial megalineations observed on unconformities A and B are evidence that an ice shelf was present in the Beaufort slope area at different times (Riedel et al., in press; Woodworth-Lynas et al., 2016a). Unconformity A lies stratigraphically between the two shallowest channel-levee sequences (Fig. 6), confirming that Kugmallit fan was active during late glacial times. Unconformity B is regionally widespread; the smoothness of this unconformity and preservation of undulating surfaces and a paleovalley 150 to 250 m below the level of megalineations (Fig. 6) indicate that this ice shelf planed off topographic highs of the paleoslope. The dominance of laminated sediments above unconformity B indicates a significant change in the depositional setting of the slope area, from a channelized-fan depositional system with high sedimentation rates fed by fluvial sources to hemipelagic deposition with lower sedimentation rates.

Rivers originating in the mountain belts of northern Yukon are thought to be the main sources of Plio–Pleistocene Iperk sedimentation (Duk-Rodkin and Hughes, 1994; Lane and Dietrich, 1995). Glacial cycles associated with the Quaternary Laurentide Ice Sheet modulated sediment input to the Beaufort shelf and slope region (Blasco et al., 1990) with potential rapid sediment influx during glacial melting. After the Last Glacial Maximum, fluvial drainage patterns were reoriented and expanded to encompass the present day Mackenzie River drainage (Duk-Rodkin and Hughes, 1994; Zazula et al., 2004). Layers deposited during the Last Glacial Maximum have been deposited above unconformity B (Blasco et al., 2013). It is possible that this unconformity correlates to the regional reorganization of river flow resulting in different depositional environments. The deepwater fan that underlies much of the Canada Basin is called the Mackenzie fan on the assumption that these sediments flowed through the Mackenzie River system. However, it now seems likely that many of the turbidite and MTD deposits (Mosher et al., 2012) imaged in the Canada Basin originated instead from the Kugmallit and Ikit fans.

Potential geohazards

Potential geohazards in marine settings typically include the occurrence of shallow gas, active faulting, weak formations, recent slope instability, and shallow water flows. In the outer Beaufort Shelf and upper slope, permafrost, permafrost gas hydrates, and conventional marine gas hydrates are also potential geohazards (Blasco et al., 2013). The channel-levee sequences making up the Kugmallit and Ikit fans show evidence of rapid deposition, localized normal and reverse faulting, and various forms of sediment instability. Extensive MTD complexes imaged in the data are the result of massive soft sediment deformation. Although the observed deformation structures do not propagate into the shallowest depositional unit, the abundance of high relief surfaces and MTDs indicate a history of repeated slope failures, as has been observed above unconformity B (Riedel et al., in press). The variable rates of deposition inferred in these settings, as well as the potential for vertical and lateral variations in permeability, create the potential for differential consolidation potentially creating overpressure conditions similar to those described by Winker and Shipp (2002). In particular, channel sands confined laterally and vertically by fine-grained sediments of the levee deposits can be overpressured, causing significant water flow when drilled. Riedel et al. (2016) noted relatively low stacking velocities associated with channel deposits. In addition, channel walls can fail inward (Sawyer et al., 2014). Overpressure can be visible as high amplitude reflections at detachment surfaces (Hubbert and Rubey, 1959; McConnell and Campbell, 2000; Bangs et al., 2004), such as underneath slide blocks in Figures 6 and 7. These sediment complexes likely contain geohazards (McConnell and Campbell, 2000) not previously described in previous assessments. Variable lithologies and associated vertical and lateral changes in permeability also create the potential for trapping shallow gas. Indeed, biogenic gas is actively discharging from the seabed in the outer shelf, and mud volcanoes on the slope are also discharging methane from depth (Paull et al., 2015). High amplitude reflections above low amplitude or non-reflective intervals are often interpreted as indicators of gas in the sediments; this combination has been observed near a mud volcano in the Ikit area (Fig. 4).

SUMMARY AND CONCLUSIONS

3-D seismic-reflection data image two slope fans on the central Beaufort slope herein called the Kugmallit fan and the Ikit fan. These features apparently emanated from different shelf-edge channel sources, but their close proximity resulted in the slope fans coalescing downslope. The reflection data provide detailed images of complex, variable and high energy clastic depositional systems in this slope fan setting, which we interpret were formed in association with high sediment input associated with Quaternary glaciations. Channel-levee complexes built out over older slope

deposits and failed laterally. Debris flows from these local sources as well as from the shelf edge flowed between the channel-levee complexes further building up the fan. Slump blocks to chaotic mass-transport deposits are common features; as are angular unconformities with local relief up to hundreds of metres. Distal turbidites and overbank deposits draped over high-relief unconformities can resemble discordant sedimentary folds in the laterally distal fan. A regional unconformity grooved by glacial megalineations indicates that an ice shelf eroded and smoothed off the top of the fan. Seafloor conformal glaciomarine and postglacial hemipelagic sediments overlie the unconformity and have smoothed the topographic signature of the fan. Laminar sediments overlying this unconformity truncate the channel-levee complexes and indicate that the sedimentary source feeding the complexes was no longer active.

Recognizing and characterizing the previously unknown slope fan complexes allows us to consider potential geohazards. Overpressure and fluid flow within the sedimentary section could create potential hazards to drilling. Highly variable sediment composition and deposition rates between glacial and interglacial cycles may have resulted in disequilibrium compaction and created overpressure in discrete intervals of the slope sections. Mud volcanoes and seismic indicators of gas show that fluids are migrating through the sediments. Abundant MTDs indicate periods of significant slope instability associated with fan development that has continued to recent times.

ACKNOWLEDGMENTS

The authors are most grateful to Imperial Oil Ltd. for access to the Ajurak 3-D seismic-reflection data set and to BP Exploration for access to the Pokak 3-D seismic-reflection data set. Discussions with P.R. Hill and E.L. King and reviews by J.R. Dietrich and K. Raines have been useful.

REFERENCES

Bangs, N.L., Shipley, T.H., Gulick, S.P.S., Moore, G.F., Kuromoto, S., and Nakamura, Y., 2004. Evolution of the Nankai Trough décollement from the trench into the seismogenic zone: inferences from three-dimensional seismic reflection imaging; Geology, v. 32, p. 273–276. https://doi.org/10.1130/G20211.2

Batchelor, C.L., Dowdeswell, J.A., and Pietras, J.T., 2013. Seismic stratigraphy, sedimentary architecture and palaeo–glaciology of the Mackenzie Trough: evidence for two Quaternary ice advances and limited fan development on the western Canadian Beaufort Sea margin; Quaternary Science Reviews, v. 65, p. 73–87. https://doi.org/10.1016/j.quascirev.2013.01.021

Batchelor, C.L., Dowdeswell, J.A., and Pietras, J.T., 2014. Evidence for multiple Quaternary ice advances and fan development from the Amundsen Gulf cross-shelf trough and slope, Canadian Beaufort Sea margin; Marine and Petroleum Geology, v. 52, p. 125–143. https://doi.org/10.1016/j.marpetgeo.2013.11.005

Blasco, S.M., Fortin, G., Hill, P.R., O'Connor, M.J., and Brigham-Grette, J., 1990. The late Neogene and Quaternary stratigraphy of the Canadian Beaufort continental shelf; *in* The Arctic Ocean region, (ed.) A. Grantz, L. Johnson, and J.F. Sweeney; Geological Society of America, The Geology of North America series, Boulder, Colorado, v. 50, p. 491–502. https://doi.org/10.1130/DNAG-GNA-L.491

Blasco, S., Bennett, R., Brent, T., Burton, M., Campbell, P., Carr, E., Covill, R., Dallimore, S., Davies, E., Hughes-Clarke, J., Issler, D., MacKillop, K., Mazzotti, S., Patton, E., Shearer, J., and White, M., 2013. 2010 state of knowledge: Beaufort Sea seabed geohazards associated with offshore hydrocarbon development; Geological Survey of Canada, Open File 6989, 340 p. https://doi.org/10.4095/292616

Cameron, G.D.M. and King, E.L., 2019. Mass-failure complexes on the central Beaufort Slope, offshore Northwest Territories; Geological Survey of Canada, Open File 8356, 39 p. https://doi.org/10.4095/314644

Dietrich, J.R., Dixon, J., and McNeil, D., 1985. Sequence analysis and nomenclature of Upper Cretaceous to Holocene strata in the Beaufort–Mackenzie basin; *in* Current Research, Part A; Geological Survey of Canada, Paper 85-1A, p. 613–628. https://doi.org/10.4095/120169

Dietrich, J., Chen, Z., Chi, G., Dixon, J., Hu, K., and McNeil, D., 2010. Petroleum plays in Upper Cenozoic strata in the Beaufort–Mackenzie basin, Arctic Canada; American Association of Petroleum Geologists International Conference and Exhibition, Calgary, Alberta, September 12–15, 2010.

Dixon, J., 1996. Geological atlas of the Beaufort–Mackenzie area; Geological Survey of Canada, Miscellaneous Report 59, 173 p. https://doi.org/10.4095/207658

Dixon, J. and Dietrich, J.R., 1990. Canadian Beaufort Sea and adjacent land areas; *in* The Arctic Ocean region, (ed.) A. Grantz, L. Johnson, and J.F. Sweeney; Geological Society of America, The Geology of North America series, Boulder, Colorado, v. 50, p. 239–256. https://doi.org/10.1130/DNAG-GNA-L

Dixon, J., Dietrich, J.R., and McNeil, D., 1992. Upper Cretaceous to Pleistocene sequence stratigraphy of the Beaufort–Mackenzie and Banks Island areas, northwest Canada; Geological Survey of Canada, Bulletin 407, 90 p. https://doi.org/10.4095/133237

Duk-Rodkin, A. and Hughes, O.L., 1994. Tertiary–Quaternary drainage of the pre-glacial Mackenzie basin; Quaternary International, v. 22-23, p. 221–241. https://doi.org/10.1016/1040-6182(94)90015-9

Dyke, A.S., Andrews, J.T., Clark, P.U., England, J.H., Miller, G.H., Shaw, J., and Veillette, J.J., 2002. The Laurentide and Innuitian ice sheets during the Last Glacial Maximum; Quaternary Science Reviews, v. 21, p. 9–31. https://doi.org/10.1016/S0277-3791(01)00095-6

Flood, R.D., Manley, P.L., Kowsmann, R.O., Appi, C.J., and Pirmez, C., 1991. Seismic facies and late Quaternary growth of Amazon submarine fan; *in* Seismic Facies and Sedimentary Processes of Submarine Fans and Turbidite Systems, (ed.) P. Weimer and M.H. Link; Frontiers in Sedimentary Geology, Springer, New York, NY, p. 415–433.

Grantz, A., May, S.D., Taylor, P.T., and Lawver, L.A., 1990. Canada Basin; *in* The Arctic Ocean region, (ed.) A. Grantz, L. Johnson, and J.F. Sweeney; Geological Society of America, The Geology of North America series, Boulder, Colorado, v. 50, p. 379–402. https://doi.org/10.1130/DNAG-GNA-L

Graves, J., Chen, Z., Dietrich, J.R., and Dixon, J., 2010. Seismic interpretation and structural analysis of the Beaufort–Mackenzie basin; Geological Survey of Canada, Open File 6217, 22 p. https://doi.org/10.4095/262724

Helwig, J., Kumar, N., Emmet, P., and Dinkelman, M.G., 2015. Regional seismic interpretation of crustal framework, Canadian Arctic passive margin, Beaufort Sea, with comments on petroleum potential; *in* Arctic Petroleum Geology, (ed.) A.M. Spencer, A.F. Embry, D.L. Gautier, A.V. Stoupakova, and K. Sørensen; Geological Society, London, Memoirs, v. 35, p. 527–543. https://doi.org/10.1144/M35.35

Hesse, R., Klauck, I., Khodabakhsh, S., and Piper, D., 1999. Continental slope sedimentation adjacent to an ice margin III: the upper Labrador Slope; Marine Geology, v. 155, p. 249–276. https://doi.org/10.1016/S0025-3227(98)00054-1

Hill, P.R., Hequette, A., and Ruz, M.-H., 1993. Holocene sea-level history of the Canadian Beaufort Shelf; Canadian Journal of Earth Sciences, v. 30, p. 103–108. https://doi.org/10.1139/e93-009

Hubbert, M.K. and Rubey, W.W., 1959. Role of fluid pressure in mechanics of overthrust faulting; Geological Society of America Bulletin, v. 70, p. 115–166. https://doi.org/10.1130/0016-7606(1959)70[115:ROFPIM]2.0.CO;2

Jakobsson, M., Grantz, A., Kristoffersen, Y., and Macnab, R., 2003. Physiographic provinces of the Arctic Ocean seafloor; Geological Society of America Bulletin, v. 115, p. 1443–1455. https://doi.org/10.1130/B25216.1

Jobe, Z.R., Lowe, D.R., and Uchytil, S.J., 2011. Two fundamentally different types of submarine canyons along the continental margin of Equatorial Guinea; Marine and Petroleum Geology, v. 28, p. 843–860. https://doi.org/10.1016/j.marpetgeo.2010.07.012

Lane, L.S. and Dietrich, J.R., 1995. Tertiary structural evolution of the Beaufort Sea – Mackenzie Delta region, Arctic Canada; Bulletin of Canadian Petroleum Geology, v. 43, p. 293–314.

Mayall, M., Jones, E., and Casey, M., 2006. Turbidite channel reservoirs – key elements in facies prediction and effective development; Marine and Petroleum Geology, v. 23, p. 821–841. https://doi.org/10.1016/j.marpetgeo.2006.08.001

McConnell, D. and Campbell, K.J., 2000. Seismic interpretation, identification of shallow water flow potential. Using high-resolution 3D and 2D; Offshore, v. 60, p. 54–56.

McNeil, D.H., Duk-Rodkin, A., Dixon, J., Dietrich, J., White, J.M., Miller, K.G., and Issler, D.R., 2001. Sequence stratigraphy, biotic change, $^{87}Sr/^{86}Sr$ record, paleoclimatic history, and sedimentation rate change across a regional late Cenozoic unconformity in Arctic Canada; Canadian Journal of Earth Sciences, v. 38, p. 309–331. https://doi.org/10.1139/e00-098

Mosher, D.C., Shimeld, J.W., Hutchinson, D., Lebedeva-Ivanova, N., and Chapman, C.B., 2012. Submarine landslides in Arctic sedimentation: Canada Basin; *in* Submarine Mass Movements and Their Consequences. Advances in Natural and Technological Hazards Research, (ed.) Y. Yamada, K. Kawamura, K. Ikehara, Y. Ogawa, R. Urgeles, D. Mosher, J. Chaytor, and M. Strasser; Springer, Dordrecht, v. 31, p. 147–157. https://doi.org/10.1007/978-94-007-2162-3_13

Murton, J.B., Bateman, M.D., Dallimore, S.R., Teller, J.T., and Yang, Z., 2010. Identification of Younger Dryas outburst flood path from Lake Agassiz to the Arctic Ocean; Nature, v. 464, p. 740–743. https://doi.org/10.1038/nature08954

Pacht, J.A., Bowen, B., Shaffer, B.L., and Pottorf, W.R., 1992. System tracts, seismic facies, and attribute analysis within a sequence-stratigraphic framework – example from the offshore Louisiana Gulf coast; *in* Marine Clastic Reservoirs, (ed.) E.G. Rhodes and T. Moslow; Frontiers in Sedimentary Geology; Springer, New York, p. 21–39. https://doi.org/10.1007/978-1-4757-0160-9_2

Paull, C.K., Dallimore, S.R., Caress, D., Gwiazda, R., Melling, H., Riedel, M., Jin, Y.K., Hong, J.K., Kim, Y.-G., Graves, D., Sherman, A., Lundsten, E., Anderson, K., Lundsten, L., Villinger, H., Kopf, A., Johnson, S.B., Hughes Clarke, J., Blasco, S., Conway, K., Neelands, P., Thomas, H., and Côté, M., 2015. Active mud volcanoes on the continental slope of the Beaufort Sea; Geochemistry, Geophysics, Geosystems, v. 16, p. 3160–3181. https://doi.org/10.1002/2015GC005928

Pelletier, B.R. (ed.), 1987. Marine science atlas of the Beaufort Sea: geology and geophysics; Geological Survey of Canada, Miscellaneous Report 40, 39 p. https://doi.org/10.4095/126940

Picard, K., 2012. Integrated modeling for stratigraphic development of the Mackenzie Trough and the eastern Beaufort Shelf, N.W.T., Canada; M.Sc. thesis, The University of Victoria, Victoria, British Columbia, 238 p.

Pickering, K.T. and Hiscott, R.N., 2016. Deep marine systems: processes, deposits environments, tectonics and sedimentation; Wiley and American Geophysical Union, Washington, D.C., 672 p.

Posamentier, H.W. and Kolla, V., 2003. Seismic geomorphology and stratigraphy of depositional elements in deep-water settings; Journal of Sedimentary Research, v. 73, p. 367–388. https://doi.org/10.1306/111302730367

Posamentier, H.W. and Martinsen, O.J., 2011. The character and genesis of submarine mass-transport deposits: insights from outcrop and 3D seismic data; *in* Mass-Transport Deposits in Deepwater Setting, (ed.) R.C. Shipp, P. Weimar, and H.W. Posamentier; SEPM Special Publication, Tulsa, USA, v. 96, p. 7–38. https://doi.org/10.2110/sepmsp.096.007

Rampton, V.N., 1988. Quaternary geology of the Tuktoyaktuk coastlands, Northwest Territories; Geological Survey of Canada, Memoir 423, 98 p. https://doi.org/10.4095/126937

Richardson, S.E.J., Davies, R.J., Allen, M.B., and Grant, S.F., 2011. Structure and evolution of mass transport deposits in the South Caspian Basin, Azerbaijan; Basin Research, v. 23, p. 702–719. https://doi.org/10.1111/j.1365-2117.2011.00508.x

Riedel, M., Hong, J.K., Jin, Y.K., Rohr, K.M.M., and Côté, M.M., 2016. First results on velocity analyses of multichannel seismic data acquired with the icebreaker RV *Araon* across the southern Beaufort Sea; Geological Survey of Canada, Current Research 2016-3, 27 p. https://doi.org/10.4095/298840

Riedel, M., King, E.L., Cameron, G.D.M., Blasco, S., Conway, K.W., Dallimore, S.R., Rohr, K.M.M., Jin, Y.K. and Hong, J.K., 2021. A chronology of post-glacial mass-transport deposits on the Canadian Beaufort Slope; Marine Geology, v. 433, no. 106407, 18 p. https://doi.org/10.1016/j.margeo.2020.106407

Riedel, M., Dallimore, S.R., Wamsteeker, M., Taylor, G., King, E.L., Hong, J.K., Jin, Y.K., in press. Large-scale lineations from a grounded ice-shelf in the Canadian Beaufort Sea. Earth and Planetary Sciences Letters.

Rydningen, T.A., Laberg, J.S., and Kolstad, V., 2016. Late Cenozoic evolution of high-gradient trough mouth fans and canyons on the glaciated continental margin offshore Troms, northern Norway — paleoclimatic implications and sediment yield; Geological Society of America Bulletin, v. 128, p. 576–596. https://doi.org/10.1130/B31302.1

Saint-Ange, F., Kuus, P., Blasco, S., Piper, D.J.W., Clarke, J.H., and MacKillop, K., 2014. Multiple failure styles related to shallow gas and fluid venting, upper slope Canadian Beaufort Sea, northern Canada; Marine Geology, v. 355, p. 136–149. https://doi.org/10.1016/j.margeo.2014.05.014

Sawyer, D.E., Flemings, P.B., Shipp, R.C., and Winker, C.D., 2007. Seismic geomorphology, lithology, and evolution of the late Pleistocene Mars–Ursa turbidite region, Mississippi Canyon area, northern Gulf of Mexico; Bulletin of the American Association of Petroleum Geologists, v. 91, p. 215–234. https://doi.org/10.1306/08290605190

Sawyer, D.E., Flemings, P.B., and Nikolinakou, M., 2014. Continuous deep-seated slope failure recycles sediments and limits levee height in submarine channels; Geology, v. 42, p. 15–18. https://doi.org/10.1130/G34870.1

Vail, P.R., 1987. Seismic stratigraphy interpretation procedure; *in* Atlas of seismic stratigraphy, (ed.) A.W. Bally; American Association of Petroleum Geologists Studies in Geology, v. 27, p. 1–10.

Vincent, J.-S., 1983. La géologie du Quaternaire et la géomorphologie de l'île Banks, Arctique canadien; Geological Survey of Canada, Memoir 405, 118 p. https://doi.org/10.4095/119517

Weimer, P. and Slatt, R.M., 2007. Introduction to the petroleum geology of deepwater settings; AAPG Studies in Geology, v. 57, Tulsa, USA. https://doi.org/10.1306/St571314

Winker, C.D. and Shipp, R.C., 2002. Sequence stratigraphic framework for prediction of shallow water flow in the greater Mars–Ursa area, Mississippi Canyon area, Gulf of Mexico continental slope; *in* Sequence stratigraphic models for exploration and production: Evolving methodology, emerging models, and application histories, (ed.) J.M. Armentrout and N.C. Rosen; SEPM Society Sedimentary Geology. https://doi.org/10.5724/gcs.02.22

Woodworth-Lynas, C. Blasco, S. Duff, D., Fowler, J., Işler, E.B., Landva, J., Cumming, E., Caines A., and Smith, C., 2016a. Geophysical and geological data compilation outer shelf and upper slope, southern Beaufort Sea: a handbook of geohazard conditions; Environmental Studies Research Fund (Canada), Report 208-1, 36 p. <https://www.esrfunds.org/sites/www.esrfunds.org/files/publications/ESRF208-1-Woodworth-Lynas-Blasco.pdf> [accessed March 31, 2021]

Woodworth-Lynas, C. Blasco, S. Duff, D., Fowler, J., Işler, E.B., Landva, J., Cumming, E., Caines, A., and Smith, C., 2016b. Geophysical and geological data compilation outer shelf and upper slope, southern Beaufort Sea: a handbook of geohazard conditions, Environmental Studies Research Fund (Canada), Report 208-2, 10 p. <https://www.esrfunds.org/sites/www.esrfunds.org/files/publications/ESRF208-2-Enclosures_Woodworth-Lynas,%20Blasco.pdf> [accessed March 31, 2021]

Zazula, G.D., Duk-Rodkin, A., Schweger, C.E., and Morlan, R.E., 2004. Late Pleistocene chronology of Lake Old Crow and the north-west margin of the Laurentide Ice Sheet; Developments in Quaternary Sciences, v. 2(B), p. 347–362. https://doi.org/10.1016/S1571-0866(04)80207-0